Au_nHg_m Clusters: Mercury Aurides, Gold Amalgams, or van der Waals Aggregates?†

Patryk Zaleski-Ejgierd and Pekka Pyykkö*

Department of Chemistry, University of Helsinki, POB 55, A. I. Virtasen aukio 1, 00014 Helsinki, Finland

Received: November 27, 2008; Revised Manuscript Received: January 13, 2009

The class of bimetallic clusters, Au_nM_m (M = Zn, Cd, Hg), is calculated at the ab initio level using the DFT, RI-MP2, and CCSD(T) methods. For the triatomic Au_2M (M = Zn, Cd), the auride-type linear Au−M−Au structures are preferred; for Au_2Hg, the linear Au−Au−Hg "amalgam" is preferred. The mixed cation $[HgAuHg]^+$, an analog of the known solid-state species Hg_3^{2+}, is predicted. For larger Au_nHg_m clusters, the results are similar to the isoelectronic Au_n^{M-} anions. Several local minima and transition states are identified. All are found to be planar.

Introduction

The structures of metal clusters are of current interest. For the gold clusters, Au_n and their ions, a large number of alternative structures are already found, as recently summarized.[1] We now consider the mixed case of neutral Au_nHg_m clusters or, in the simplest triatomic case, the Au_2M systems (M = Zn, Cd, Hg).

The simple diatomic closed-shell species, $AuHg^+$, was considered by Wesendrup et al.[2] Perhaps the best calibration calculations on the isoelectronic Au_2 are those by Hess and Kaldor[3] or by Lee et al.[4] The bimetallic Au_nZn clusters and their ions were studied by Tanaka et al.[5,6] Rykova et al.[7] treated Au_nM (M = Hg, E112). An experimental gas-phase study of the photoelectron spectra of Au_nZn was presented by Koyasu et al.[8] The closed-shell pure mercury chain cations Hg_2^{2+}, Hg_3^{2+}, and Hg_4^{2+} are known in solids.[9−12] We now propose the possible mixed isoelectronic species $[HgAuHg]^+$. The inverted case, a triatomic two-valence-electron $[AuHgAu]^{2+}$, was synthesized in a solid by Catalano et al.[13]

One question is whether the diaurides, $Au-M_m-Au$, or the "digold amalgam molecules", $Au-Au-M_m$, will be preferred. A further question is that of planarity versus nonplanarity[14] for these metal clusters. (See ref 1 for the literature on Au_n.) The presented systems have five atoms or less, and they all turn out to be planar, as the Au_n clusters in this size range. Selected possible structures of the present species are shown in Figure 1.

Computational Methods

All systems were calculated with density functional theory (DFT) using the TPSS exchange−correlation functional[15−18] and the second-order Møller−Plesset perturbation theory (MP2) with the resolution of identity (RI).[19] TPSS was chosen on the basis of the CCSD(T) benchmarks. The DFT/RI-MP2 part of the reported calculations was performed using the TURBOMOLE (v. 5.10) program package.[20] Because of the presence of possible metallophilic interactions between all pairs of neighboring atoms, selected two- and three-atomic model systems were calculated using the coupled-cluster method, (CCSD(T)), with single, double, and perturbative triple excitations. The DFT methods typically underbind such partially metallophilic systems and the RI-MP2 method typically overbinds, whereas CCSD(T) is a reliable benchmark method for single-configuration-dominated systems. The coupled-cluster results were obtained using the MOLPRO program package.[21] All clusters were treated as singlet, closed-shell species. The T1 amplitude analysis indicated no significant multiconfiguration contributions.

For both DFT and RI-MP2 calculations, recent Karlsruhe, quadruple-ζ-with-polarization (def2-QZVPP) basis sets were employed.[22] The corresponding auxiliary bases were used for RI-MP2. During the initial investigation, we used smaller, triple-ζ-with-polarization (def2-TZVPP) bases.[22] We found that although the TZVPP bases yield similar geometries as the QZVPP ones, the calculated vibrational spectra differed, especially in the low-frequency range, including the sign: some shallow minima at TZVPP level were transformed to transition states at QZVPP. Therefore, larger quadruple-ζ quality bases were applied throughout the calculations. For DFT and RI-MP2 calculations, we used the 19-valence-electron (19-VE) effective core potentials (ECP) of Andrae et al.[23] for gold; similarly, for mercury and cadmium, the 20-VE ECPs were used to account for scalar relativistic effects.[23] In these lower-level calculations, zinc was treated at the nonrelativistic all-electron level.[22] During the coupled-cluster calculation, augmented triple-ζ correlation-consistent (aug-cc-pVTZ-PP) basis sets of Peterson and Puzzarini[24] were used with the 19-VE ECP for gold and the 20-VE ECPs of Figgen et al.[25] for Hg, Cd, and Zn.

During the post-Hartree−Fock calculations, all explicitly treated electrons were correlated, and no virtual molecular orbitals were frozen. In other recent work on the structures of the triatomic coinage-metal cyanides,[26] M′CN, and on the basis-set limit of the aurophilic attraction,[27] we used combinations of both types of bases and ECPs[22−25] with excellent results.

To identify possible local minima, we considered a large number of starting geometries, including linear, planar, and nonplanar. All were optimized within the C_1 symmetry with no symmetry constraints imposed. In Figure 1, we present several initial or resulting schematic conformations. All of the starting 3D structures converged to one of the 2D minima in Figure 1.

To distinguish a local minimum from a transition state, we performed a vibrational analysis. For each of the DFT, MP2, and CCSD(T) methods, the numerical harmonic vibrational spectra were calculated.

To estimate the probability of the formation of the various clusters, we calculated formation energies of the energetically

† Part of the special issue "Russell M. Pitzer Festschrift".

* Corresponding author. E-mail: pekka.pyykko@helsinki.fi.

10.1021/jp810423j CCC: $40.75
Published on Web 02/19/2009

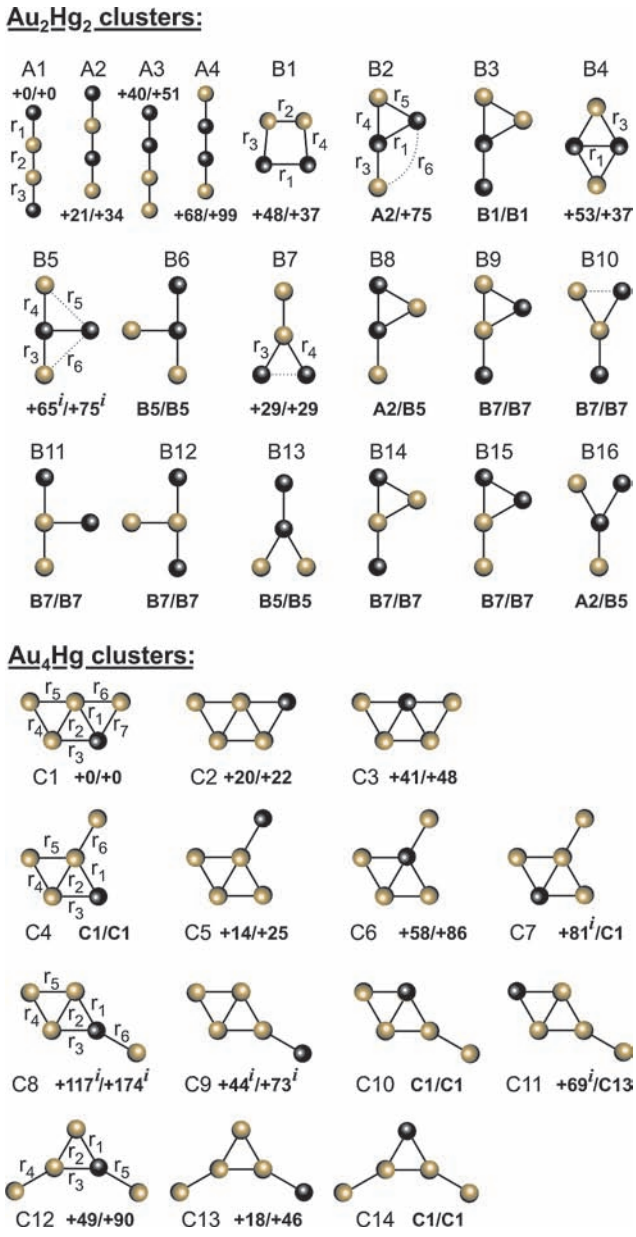

Figure 1. Schematic representation of selected investigated structures. The relative energy (kJ mol^{-1}) with respect to the energetically lowest structure is given below each structure. The two energies are given at DFT/MP2 levels, respectively. Black spheres are mercury atoms, whereas yellow spheres are gold. *i* indicates a transition state.

lowest-lying isomers. The relative energies of remaining isomers are given for comparison.

Results and Discussion

Preferred Geometries. ***Au_2M, M = Zn, Cd, Hg.*** These neutral triatomic species and the experimentally known isoelectronic ions were calculated using the DFT, RI-MP2, and CCSD(T) methods. The calculated results are given in Tables 1 and 2.

In general, for triatomic A_2B species, three types of arrangement are possible: two linear and one triangular. During the optimization, linear conformations were always preferred. The relative energies of the Au−Au−M and Au−M−Au linear arrangements actually depend on M. For zinc and cadmium, structures with terminal gold atoms are preferred. On the contrary, mercury prefers to bind to the end of a Au_2 unit. This

TABLE 1: Calculated DFT, RI-MP2, and CCSD(T) Bond Lengths (pm) and Frequencies, ω (cm^{-1}), of the Reference Au_2, the Mercury-Containing Cations, and the Au_4^{2-} Anion[a]

	TPSS QZVPP	RI-MP2 QZVPP	CCSD(T) AVT	exptl
	Au−Au			
r(Au−Au)	250.54	242.73	248.38	247.19[b]
(σ_g) ω_1	179.3	209.4	190.1	190.9[b]
	$[Hg-Au-Hg]^+$			
r(Hg−Au)	266.28	259.01	257.59	
(σ_u) ω_1	166.7	195.8	179.1	
(σ_g) ω_2	79.3	91.6	108.7	
(π_g) ω_3	21.2	26.5	30.7	
	$[Hg-Hg-Hg]^{2+}$			
r(Hg−Hg)	268.28	256.10	262.03	255.20[c]
(σ_u) ω_1	153.4	195.6	177.9	
(σ_g) ω_2	88.9	114.8	103.3	
(π_g) ω_3	31.8	40.5	35.2	
	Au_2Hg^{2+} ($D_{\infty h}$)			
r(Au−Hg)	269.41	265.51		278[d]
(σ_u) ω_1	127.1	114.9		
(σ_g) ω_2	79.4	79.6		
(π_g) ω_3	12.7	8.1		
	Au_2Hg^{2+} (C_{2v})			
r(Au−Au)	264.87	264.87		
r(Au−Hg)	269.52	259.40		
ω_1	150.8	174.8		
ω_2	108.9	122.0		
ω_3	84.8	106.5		
	$[Hg-Hg-Hg-Hg]^{2+}$			
(central)r(Hg−Hg)	272.14	254.99		259[e]
(terminal)r(Hg−Hg)	267.99	260.22		262[e]
	$[Au-Au-Au-Au]^{2-}$			
(central)r(Au−Au)	259.38	249.68		
(terminal)r(Au−Au)	266.83	257.13		

[a] See the text for discussion on this dianion. [b] Ref 28. [c] In solid $Hg_3(AsF_6)_2$, ref 34. [d] Ref 13. [e] Ref 11.

trend is the same for all methods used. These two cases could be called Zn and Cd diaurides and a molecular gold amalgam, respectively. Note that the ionization potentials (IP) of Zn, Cd, and Hg are 9.39, 8.99, and 10.44, respectively.[28] The large IP of Hg is due to relativity. It makes the ionization of Hg the hardest, even in a chemical sense.

In the case of Au−Au−M conformations, the Au−Au distances are practically constant for different M and only slightly longer (by 2 to 3 pm) than those in isolated Au_2. In the Au−M−Au isomers, the Au−M distances are shorter than in the Au−Au−M counterparts by ∼8−10 pm. Going from zinc to cadmium, the Au−M distance increases significantly by ∼20 pm, whereas going from cadmium to mercury, there is practically no increase in the bond length. This is yet another example of the relativistic bond-length contraction.

In addition to neutral species, the cationic, two-valence-electron $[AuHgAu]^{2+}$ was also calculated because it is experimentally known in solid state[13] and may serve as benchmark. The structure is linear (r_{Au-Hg}: 278 pm (exptl), 269 pm (free-ion DFT)). The calculated free ion actually prefers a C_{2v} triangular structure by ∼58 and ∼78 kJ mol^{-1} at DFT and RI-MP2 levels, respectively.

We note a very good agreement between the DFT/TPSS results and the computationally much more expensive CCSD(T) results. On the basis of the current results and our earlier experience, we expect that the applied DFT method is both qualitatively and quantitatively reliable for predicting new predominantly covalently bound Au_nHg_m clusters.

TABLE 2: Calculated DFT, RI-MP2, and CCSD(T) Bond Lengths (pm), Harmonic Frequencies, ω (cm^{-1}), Dipole Moments, μ [Debye], and the Total Energy Differences, ΔE (kJ mol^{-1}), of the Three-Atom Au_2M Clusters

	TPSS QZVPP	RI-MP2 QZVPP	CCSD(T) AVT	TPSS QZVPP	RI-MP2 QZVPP	CCSD(T) AVT	TPSS QZVPP	RI-MP2 QZVPP	CCSD(T) AVT
		Au−Au−Zn			Au−Au−Cd			Au−Au−Hg	
ΔE^a	−109	−141	−101	−91	−118	−92	−66	−103	−72
r_1(Au−Au)	253.48	244.86	250.61	253.12	244.3	250.33	252.01	243.32	249.14
r_2(Au−M)	241.06	235.52	240.17	260.10	253.3	258.93	265.00	257.16	263.92
μ	3.66	4.69		3.98	4.63		2.83	3.26	
(σ) ω_1	214.0	242.0	216.5	189.7	221.3	199.3	187.5	220.6	199.3
(σ) ω_2	147.6	173.4	155.8	122.5	140.8	126.9	98.6	112.2	100.0
(π) ω_3	30.8	48.7	34.6	29.6	37.2	30.6	26.0	35.8	30.4
		Au−Zn−Au			Au−Cd−Au			Au−Hg−Au	
ΔE^a	−174	−219	−166	−124	−149	−132	−51	−75	−51
r_1(Au−M)	235.64	228.7	232.78	252.85	245.0	250.13	255.26	246.3	252.09
(σ_u) ω_1	321.7	369.9	340.6	243.9	283.6	262.6	205.2	242.7	220.3
(σ_g) ω_2	122.4	139.4	131.1	115.4	134.9	124.6	118.0	142.1	128.2
(π_g) ω_3	59.9	72.2	65.7	44.7	50.7	49.5	40.6	48.1	44.4

[a] $\Delta E = E(MAu_2) - E(Au_2) - E(M)$.

TABLE 3: Calculated DFT, RI-MP2, and CCSD(T) Bond Lengths (pm), Harmonic Frequencies, ω (cm^{-1}), Dipole Moments, μ [Debye], and the Total Energy Differences, ΔE (kJ mol^{-1}), of the Linear Four-Atomic Au_2Hg_2 Clusters[a]

case A1	TPSS QZVPP	RI-MP2 QZVPP	case A2	TPSS QZVPP	RI-MP2 QZVPP
	Hg−Au−Au−Hg			Hg−Au−Hg−Au	
ΔE^b	−185	−192			
ΔE^c	−70	−117			
ΔE^d	−55	−89			
ΔE^e	+0	+0	ΔE^e	+21	+34
r_1(Hg−Au)	267.75	259.73	r_1(Hg−Au)	270.56	262.21
r_2(Au−Au)	253.54	244.13	r_2(Au−Hg)	257.67	248.29
			r_3(Hg−Au)	256.59	247.61
μ	0.0	0.0	μ	2.97	3.45
(σ) ω_1	188.1	222.6	(σ) ω_1	199.2	237.1
(σ) ω_2	111.7	128.6	(σ) ω_2	130.0	154.5
(σ) ω_3	73.6	85.7	(σ) ω_3	75.9	90.1
(π) ω_4	31.5	39.3	(π) ω_4	45.1	56.9
(π) ω_5	11.8	17.0	(π) ω_5	13.2	21.0
case A3	TPSS QZVPP	RI-MP2 QZVPP	case A4	TPSS QZVPP	RI-MP2 QZVPP
	Hg−Hg−Au−Au			Au−Hg−Hg−Au	
ΔE^e	+40	+51	ΔE^e	+68	+99
r_1(Hg−Hg)	301.33	288.31	r_1(Au−Hg)	256.88	247.51
r_2(Hg−Au)	262.73	254.53	r_2(Hg−Hg)	267.36	255.36
r_3(Au−Au)	252.43	243.81			
μ	4.98	5.48	μ	0.0	0.0
(σ) ω_1	188.9	223.1	(σ) ω_1	197.1	240.5
(σ) ω_2	112.3	131.3	(σ) ω_2	159.7	192.3
(σ) ω_3	43.3	53.7	(σ) ω_3	78.2	99.4
(π) ω_4	32.7	44.0	(π) ω_4	53.6	65.2
(π) ω_5	8.2	13.4	(π) ω_5	21.2	24.9

[a] For bonding notation, see Figure 1. [b] $\Delta E = E(Hg_2Au_2) - E(Au_2) - 2E(Hg)$. [c] $\Delta E = E(Hg_2Au_2) - E(Au-Hg-Au) - E(Hg)$. [d] $\Delta E = E(Hg_2Au_2) - E(Au-Au-Hg) - E(Hg)$. [e] Total energy difference calculated with respect to the A1 isomer.

Au_2Hg_2. The results for these four-atom clusters are given in Tables 3 and 4. Only the DFT and RI-MP2 methods were employed because the CCSD(T) becomes too expensive for scanning the potential energy surface (PES) for a rapidly increasing number of local minima.

For the Au_2Hg_2, four linear and several further planar local minima were identified, with the linear A1 being energetically most favored for both DFT and RI-MP2. A direct structural comparison of A1 (Hg−Au−Au−Hg) with the triatomic Au−Au−Hg reveals only a small elongation of both Au−Au and Au−Hg types of bonds. In other words, the $D_{\infty h}$ "amalgam" Hg−Au−Au−Hg is preferred, and the $D_{\infty h}$ mercurous diauride Au−Hg−Hg−Au lies highest. Both lower ($C_{\infty v}$) symmetry cases, A2 and A3, have intermediate energies.

In the case of A2 (Hg−Au−Hg−Au), one can distinguish a tightly bound Au−Hg−Au "core" and a mercury atom more weakly bound to it.

The A1 (Hg−Au−Au−Hg) and A3 (Hg−Hg−Au−Au) structures can be directly compared. In both cases, the Au−Au−Hg core appears to be only slightly perturbed by the presence of additional Hg atom. Note that in A3 the DTF r(Hg−Hg) is 13 pm longer than the MP2 one. In structure A4, the r(Hg−Hg) distance is considerably shorter and typical of mercurous compounds. Therefore, the A3 should be considered a rather weak Hg···Hg−Au−Au vdW complex. The particularly low ω_{3-5} frequencies for A3 support the observation.

During the geometry scan, several planar local minima were identified, with Y-shaped B7 being the most stable. (See Figure 1). The B7 structure is remarkable in having an essentially undeformed Au_2 unit with two Hg atoms coordinated to it at a large distance from each other. It may deserve further study at much deeper levels.

Among the planar Au_2Hg_2 structures, the B5 is a C_{2v} transition state with a Hg atom loosely bound to the Au−Hg−Au chain. The Au−Hg distances in this chain are practically identical to that in the isolated Au−Hg−Au unit.

The B4 cluster adopts a D_{2h} local minimum. It is a rhomboid with four equivalent Au−Hg bonds. The Hg−Hg distance is rather long, and the Au−Au distance is even longer.

The starting point structure B2 goes over to the linear A2 at TPSS level but remains a C_s local minimum at MP2 level. The structure is actually very similar to the B5 transition state but with no imaginary frequencies observed.

Our search for nonplanar Au_2Hg_2 local minima yielded none.

Au_4^{2-} and Congeners. In addition to the Au_2Hg_2, the isoelectronic Au_4^{2-} species was also investigated. We are not proposing it as a new gas-phase species but rather as a possible anion in alkali aurides, alkali solutions in liquid ammonia, or similar reducing surroundings. Some occupied MOs of the free ion will then have positive energies, corresponding to continuum states. Continuum dissolution can, however, be prevented experimentally by counterion stabilization and computationally by the finite basis, as discussed by Pyykkö and Zhao.[29] That is

TABLE 4: Calculated DFT, RI-MP2, and CCSD(T) Bond Lengths (pm), Harmonic Frequencies, ω (cm^{-1}), Dipole Moments, μ [Debye], and the Total Energy Differences, ΔE (kJ mol^{-1}), of the Planar Four-Atomic Au_2Hg_2 Clusters[a]

case	TPSS QZVPP	RI-MP2 QZVPP	TPSS QZVPP	RI-MP2 QZVPP	TPSS QZVPP	RI-MP2 QZVPP	TPSS QZVPP	RI-MP2 QZVPP	TPSS QZVPP	RI-MP2 QZVPP
	case B1		case B2		case B4		case B5		case B7	
ΔE^b	+48	+37	→ A2	+75	+53	+37	+65[c]	+75[c]	+29	+29
r_1(Hg−Hg)	309.37	288.76		299.77	333.01	323.53	323.18	296.82	377.91	344.00
r_2(Au−Au)	256.99	249.14			429.19	408.56			252.98	244.10
r_3(Hg−Au)	277.47	263.35		245.93	271.62	260.57	255.30	246.09	274.59	264.43
r_4(Hg−Au)	277.66	268.39		246.31			255.29	246.09	274.60	265.35
r_5(Hg−Au)	395.21	355.09		331.61			414.80	376.00		
r_6(Hg−Au)	396.11	398.85		421.35			413.40	376.03		
μ	1.09	1.34		0.11	0.0	0.0	0.40	0.49	2.34	2.69
ω_1	154.7	180.4		243.1	123.8	155.0	202.5	243.3	178.2	215.6
ω_2	93.4	120.7		143.1	120.9	148.7	117.4	143.2	84.2	102.8
ω_3	86.7	105.4		64.1	111.1	137.5	41.7	68.0	83.5	97.6
ω_4	44.8	70.3		46.1	68.3	97.6	41.6	45.7	32.2	36.3
ω_5	19.5	25.8		31.1	46.5	51.7	25.4	28.7	23.4	28.7
ω_6	12.5	15.9		11.0	31.7	40.5	−4.6	−6.2	15.2	8.6
	case B3		case B6		case B8		case B9		case B10	
	→ B1	→ B1	→ B5	→ B5	→ A2	→ B5	→ B7	→ B7	→ B7	→ B7
	case B11		case B12		case B13		case B14		case B15	
	→ B7	→ B7	→ B7	→ B7	→ B5	→ B5	→ B7	→ B7	→ B7	→ B7
	case B16									
	→ A2	→ B5								

[a] Arrow sign (→) indicates a change of structure during optimization. [b] Total energy difference calculated with respect to the A1 isomer. [c] Transition state.

a good approximation for stiff, multiply bonded polyanions. Softer moieties may show larger deformations because of counterions. Indeed, when monovalent group 1 or divalent group 2 countercations are added to Au_4^{2-}, it changes shape to bent or quadratic structures.[30,31] The experimental photo electron spectrum[32] of Au_4Na^- supports a planar C_{2v} structure resembling our C3 in Figure 1. Concerning Au_4^{2-} at the DFT level, a linear $D_{\infty h}$ isomer was found to be energetically lowest, with the D_{3h} 'star' (r_{Au-Au} = 266.88 pm) and the D_{4h} square (r_{Au-Au} = 269.07 pm) higher by ∼80 and ∼130 kJ mol^{-1}, respectively. At the RI-MP2 level, a linear isomer was still favored, now followed by a C_{2v} rhombus (r_{Au-Au} = 258.03 pm, ∠ = 82.9°) and the D_{3h} star (r_{Au-Au} = 256.15 pm) higher by ∼72 and ∼84 kJ mol^{-1}, respectively.

In the case of the isoelectronic Hg_4^{2+} ion, a $D_{\infty h}$ linear isomer was found to be energetically preferred at DFT and RI-MP2 levels. The D_{3h} isomer lies higher by ∼114 and ∼93 kJ mol^{-1} and the D_{4h} square by ∼65 and ∼65 kJ mol^{-1}, respectively.

Concerning the structures, both the Hg_4^{2+} and the isoelectronic Au_4^{2-} chains have shorter bonds at the ends compared with those at the middle in both our free-molecule calculations and the solid-state experiment for Hg_4^{2+}.[11] (See Table 1.) The differences between terminal and central bond lengths at the MP2 level are 5.2 and 7.5 pm for Hg_4^{2+} and Au_4^{2-}, respectively. Note that in a simple, four-atom, six-electron Hückel model (here for one 6s orbital per atom), the 1−2 and 2−3 bond orders are 0.448 and 0.724, indeed predicting a stronger and shorter bond in the middle.

Au_4Hg. In the case of Au_4Hg, a number of local minima were identified. The results are given in Table 5. We performed an extensive search for nonplanar isomers but again found only strictly planar geometries. The structure C1, in which a mercury atom is bound to three adjacent gold atoms, emerged as the energetically most preferable. It is qualitatively similar to the structure of the isoelectronic Au_5^-.[33] The other "half-cake" structures, C2 and C3, do not lie much higher. Alternatively, one could see C2 as a neutral Au_4 (D_{2h}) with a side-on coordinated atom. Varying the coordination site gives C5 and C9. The C_{2v} structure C6 lies slightly above C3. All of the structures could be systematically grouped as follows.

The first family consists of the C1, C4, and C8 structures and the C8-related C12. Structure C4 rearranges into C1 during the optimization, and C8 is found to be an energetically high-lying transition state. The C12 isomer, in which one gold atom is separated from a rhomboidal core, lies higher in energy but has no imaginary frequencies. In all cases, the Au−Au and Au−Hg distances are typical of covalent bonds.

The second family, composed of C2, C5, C9, and C9-derived C13, possesses a rhomboidal Au_4 core. Excluding C9, the remaining structures are vibrationally stable and energetically not far from the most stable C1. The comparison of C2, C5, and C9 shows that the geometry of the rhomboidal Au_4 core is only slightly perturbed by the mercury atom. In the isolated Au_4 unit (D_{2h}), the Au−Au distances are 267.28 and 258.47 pm at DFT and RI-MP2 levels of theory respectively. Structures C5 and C2 are similar, but in the later case, the Hg···Au metallophilic attraction is strong enough to bend the r_6(Au−Hg) bond of the C2 system in the direction of the neighboring Au atom to form an additional loose bond r_7(Au−Hg). The fact that the Au−Hg bonds in C2 have different lengths by 30 pm at the RI-MP2 level supports the explanation.

The third column of Figure 1 has the unstable C10 and C14 and the already discussed C3 and C6. Finally, structures C7 and C13 are also unstable or identified as high-lying transition states, depending on the method.

Total Energies. The likely ways of making these species may involve highly nonequilibrium conditions. Nevertheless, it is interesting to consider the relative energies.

Three-Atom Species. The formation energies in Table 2 are calculated with respect to Au_2 and isolated metal atoms, M. The main observation is that mercury prefers a terminal position, as in Au−Au−M, rather than the central one. For zinc and cadmium, an insertion into the Au−Au bond is energetically preferred.

Four-Atom Au_2Hg_2 Clusters. Several formation/fragmentation channels are possible: (a) The formation energies are

TABLE 5: Calculated DFT, RI-MP2, and CCSD(T) Results of the Planar Five-Atomic Au_4Hg Clusters[a]

	TPSS QZVPP	RI-MP2 QZVPP		TPSS QZVPP	RI-MP2 QZVPP		TPSS QZVPP	RI-MP2 QZVPP		TPSS QZVPP	RI-MP2 QZVPP
case C1			case C2			case C3			case C5		
ΔE[b]	−360	−364									
ΔE[c]	−245	−289									
ΔE[d]	−230	−261									
ΔE[e]	−83	−146									
ΔE[f]	+0	+0	ΔE[f]	+20	+22	ΔE[f]	+41	+48	ΔE[f]	+14	+25
r_1(Hg−Au)	298.58	289.02	r_1(Au−Au)	272.80	265.50	r_1(Hg−Au)	295.5	288.2	r_1(Au−Au)	269.97	260.17
r_2(Au−Au)	277.21	267.67	r_2(Au−Au)	263.35	257.39	r_2(Hg−Au)	296.0	288.4	r_2(Au−Au)	261.61	252.92
r_3(Hg−Au)	266.84	256.70	r_3(Au−Au)	265.56	255.55	r_3(Au−Au)	260.5	251.5	r_3(Au−Au)	265.41	257.41
r_4(Au−Au)	263.04	254.82	r_4(Au−Au)	270.57	262.88	r_4(Au−Au)	270.8	260.3	r_4(Au−Au)	265.41	257.41
r_5(Au−Au)	261.69	252.68	r_5(Au−Au)	262.39	251.56	r_5(Hg−Au)	259.8	250.9	r_5(Au−Au)	269.99	260.17
r_6(Au−Au)	256.41	247.57	r_6(Hg−Au)	267.13	257.22	r_6(Hg−Au)	259.8	251.0	r_6(Hg−Au)	264.99	254.83
r_7(Hg−Au)	283.17	271.56	r_7(Hg−Au)	321.37	289.93	r_7(Au−Au)	270.7	260.3			
μ	0.92	1.40	μ	1.76	1.80	μ	1.82	2.17	μ	2.72	3.00
ω_1	186.9	221.8	ω_1	178.0	210.2	ω_1	187.6	217.7	ω_1	180.3	213.4
ω_2	146.1	171.7	ω_2	154.5	180.0	ω_2	149.9	177.6	ω_2	153.8	182.2
ω_3	128.4	153.1	ω_3	116.2	134.0	ω_3	125.8	149.9	ω_3	114.9	135.8
ω_4	96.6	114.7	ω_4	95.6	108.5	ω_4	100.0	127.0	ω_4	101.9	122.1
ω_5	86.7	104.8	ω_5	75.9	85.2	ω_5	86.4	103.6	ω_5	85.6	101.2
ω_6	62.6	77.2	ω_6	67.4	83.2	ω_6	41.9	48.1	ω_6	64.7	74.1
ω_7	45.6	52.4	ω_7	32.7	40.9	ω_7	35.4	39.6	ω_7	37.2	39.6
ω_8	33.9	40.5	ω_8	19.8	37.8	ω_8	27.0	25.8	ω_8	23.9	27.7
ω_9	28.9	39.3	ω_9	8.2	28.7	ω_9	22.9	23.0	ω_9	13.2	8.8
case C6			case C12			case C13			other isomers		
ΔE[f]	+58	+86	ΔE[f]	+49	+90	ΔE[f]	+18	+46			
r_1(Hg−Au)	283.36	270.80	r_1(Hg−Au)	266.40	256.66	r_1(Au−Au)	259.36	250.14			
r_2(Hg−Au)	265.94	257.29	r_2(Au−Au)	262.50	253.99	r_2(Au−Au)	265.24	256.73	C4	→ C1	→ C1
r_3(Au−Au)	260.67	252.68	r_3(Hg−Au)	272.88	262.58	r_3(Au−Au)	268.41	260.04			
r_4(Au−Au)	260.62	252.68	r_4(Au−Au)	251.88	243.67	r_4(Au−Au)	251.99	244.01	C7	+80[g]	→ C1
r_5(Hg−Au)	283.33	270.81	r_5(Hg−Au)	254.31	254.17	r_5(Hg−Au)	264.70	255.21			
r_6(Hg−Au)	254.91	245.67									
μ	0.63	0.52	μ	2.74	3.08	μ	5.21	5.81	C8	+117[g]	+174[g]
ω_1	193.7	229.8	ω_1	205.8	243.8	ω_1	201.9	236.7			
ω_2	169.8	196.7	ω_2	186.7	220.7	ω_2	167.6	199.0	C9	+44[g]	+73[g]
ω_3	135.1	159.7	ω_3	120.1	142.8	ω_3	112.3	131.3			
ω_4	83.6	95.9	ω_4	91.4	110.3	ω_4	92.4	110.7	C10	→ C1	→ C1
ω_5	70.3	94.2	ω_5	84.3	102.6	ω_5	85.2	99.9			
ω_6	49.8	63.0	ω_6	39.7	45.8	ω_6	37.9	43.6	C11	+69[g]	→ C13
ω_7	41.0	46.7	ω_7	34.9	43.6	ω_7	26.0	33.3			
ω_8	28.1	31.8	ω_8	30.4	32.2	ω_8	25.0	25.6			
ω_9	14.7	16.8	ω_9	14.6	16.0	ω_9	12.8	10.4	C14	→ C1	→ C1

[a] Arrow sign (→) indicates a change of structure during optimization. [b] $\Delta E = E(Au_4Hg) - 2E(Au_2) - E(Hg)$, [c] $\Delta E = E(Au_4Hg) - E(Au-Hg-Au) - E(Hg)$. [d] $\Delta E = E(Au_4Hg) - E(Au-Au-Hg) - E(Hg)$. [e] $\Delta E = E(Au_4Hg) - E(Au_4) - E(Hg)$. [f] Total energy difference calculated with respect to the C1 isomer. [g] Transition state.

calculated with respect to monatomic mercury and Au_2. (b) The formation of the Au_2Hg_2 species is defined with respect to Au_2, reacting with diatomic Hg_2. Because mercury is known to form a monatomic vapor at low pressures, this reaction is not considered. (c) The formation of Au_2Hg_2 is based on a reaction of a triatomic Au_2Hg unit with a Hg atom. We calculated the $Au_2Hg + Hg \rightarrow Au_2Hg_2$ formation energies with respect to both Au−Hg−Au and Au−Au−Hg. Both are exothermic, with the first being ∼20% more favored. The results are given in Tables 3 and 4.

Five-Atom Au_4Hg Clusters. Similar to the smaller clusters, a number of potential formation schemes can be proposed: (a) a reaction of a Hg with two Au_2 units, (b) a reaction of Au_2Hg (both Au−Hg−Au or Au−Au−Hg) with the Au_2 unit, and (c) a reaction of the rhombus, Au_4, unit with a Hg atom. Results are given in Table 5. Of the proposed formation cycles, a is the most exothermic and b is energetically comparable. The lowest energy gain is calculated for c because the Au_4 rhombus is already present. The calculated ΔE for $2Au_2 \rightarrow Au_4$ is −277 and −218 kJ mol^{-1} at DFT and RI-MP2 levels, respectively.

Conclusions

Some key conclusions are: (1) Whereas M = Zn and Cd prefer the linear diauride structures Au−M−Au, the case of M = Hg prefers the end-on "amalgam" Au−Au−Hg. All of these suggested species are new. (2) The ground state of Au_2Hg_2 is the linear "amalgam" Hg−Au−Au−Hg. The rather low-lying C_{2v} structure B7 may also deserve further attention. The isolated isoelectronic Au_4^{2-} has the same linear $D_{\infty h}$ structure. (3) The mixed species $[HgAuHg]^+$ is predicted. It would be an analog of the known solid-state species Hg_3^{2+}. (4) The higher energy isomer A3, the one with a loosely bound Hg, could be described as a van der Waals aggregate. (5) The lowest-energy five-atomic Au_4Hg structure is the planar C_s "half-cake" structure C1. (6) Analogous with the pure-gold systems Au_n for $n \leq 5$, all present structures were planar.

Acknowledgment. We belong to the Finnish Centre of Excellence (CoE) in Computational Molecular Science (2006−2011). We acknowledge the Centre of Scientific Com-

puting (CSC, Espoo, Finland) for providing computer resources. P.Z.-E. is supported by the Magnus Ehrnrooth Foundation.

References and Notes

(1) Pyykkö, P. *Chem. Soc. Rev.* **2008**, *37*, 1967–1997.
(2) Wesendrup, R.; Laerdahl, J. K.; Schwerdtfeger, P. *J. Chem. Phys.* **1999**, *110*, 9457–9462.
(3) Hess, B. A.; Kaldor, U. *J. Chem. Phys.* **2000**, *112*, 1809–1813.
(4) Lee, H.-S.; Han, Y.-K.; Kim, M. C.; Bae, C.; Lee, Y. S. *Chem. Phys. Lett.* **1998**, *293*, 97–102.
(5) Tanaka, H.; Neukermans, S.; Janssens, E.; Silverans, R. E.; Lievens, P. *J. Am. Chem. Soc.* **2003**, *125*, 2862–2863.
(6) Tanaka, H.; Neukermans, S.; Janssens, E.; Silverans, R. E.; Lievens, P. *J. Chem. Phys.* **2003**, *119*, 7115–7123.
(7) Rykova, E. A.; Zaitsevskii, A.; Mosyagin, N. S.; Isaev, T. A.; Titov, A. V. *J. Chem. Phys.* **2006**, *125*, 241102.
(8) Koyasu, K.; Naono, Y.; Akutsu, M.; Mitsui, M.; Nakajima, A. *Chem. Phys. Lett.* **2006**, *422*, 62–66.
(9) Gillespie, R. J.; Granger, P.; Morgan, K. R.; Schrobilgen, G. J. *Inorg. Chem.* **1984**, *23*, 887–891.
(10) Kertesz, M.; Guloy, A. M. *Inorg. Chem.* **1987**, *26*, 2852–2857.
(11) Cutforth, B. D.; Gillespie, R. J.; Ireland, P.; Sawyer, J. F.; Ummat, P. K. *Inorg. Chem.* **1983**, *22*, 1344–1347.
(12) Brown, I. D.; Gillespie, R. J.; Morgan, K. R.; Sawyer, J. F.; Schmidt, K. J.; Tun, Z.; Ummat, P. K. *Inorg. Chem.* **1987**, *26*, 689–693.
(13) Catalano, V. J.; Malwitz, M. A.; Noll, B. C. *Chem. Commun.* **2001**, 581–582.
(14) Johansson, M. P.; Lechtken, A.; Schooss, D.; Kappes, M. M.; Furche, F. *Phys. Rev. A* **2008**, *77*, 053202.
(15) Dirac, P. A. M. *Proc. Royal Soc. London* **1929**, *A123*, 714–733.
(16) Slater, J. C. *Phys. Rev.* **1951**, *81*, 385–390.
(17) Perdew, J. P.; Wang, Y. *Phys. Rev. B* **1992**, *45*, 13244–13249.
(18) Tao, J.; Perdew, J. P.; Staroverov, V. N.; Scuseria, G. E. *Phys. Rev. Lett.* **2003**, *91*, 146401.
(19) Hättig, C.; Köhn, A.; Hald, K. *J. Chem. Phys.* **2002**, *116*, 5401–5410.
(20) Ahlrichs, R.; Bär, M.; Häser, M.; Horn, H.; Kölmel, C. *Chem. Phys. Lett.* **1989**, *162*, 165–169.
(21) Werner, H.-J.; Knowles, P. J.; Lindh, R.; Manby, F. R.; Schütz, M.; et al. *MOLPRO: A Package of Ab Initio Programs*, version 2008.1, http://www.molpro.net.
(22) Weigend, F.; Ahlrichs, R. *Phys. Chem. Chem. Phys.* **2005**, *7*, 3297–3305.
(23) Andrae, D.; Häussermann, U.; Dolg, M.; Stoll, H.; Preuss, H. *Theor. Chim. Acta* **1990**, *77*, 123–141.
(24) Peterson, K. A.; Puzzarini, C. *Theor. Chem. Acc.* **2005**, *114*, 283–296.
(25) Figgen, D.; Rauhut, G.; Dolg, M.; Stoll, H. *Chem. Phys.* **2005**, *311*, 227–244.
(26) Zaleski-Ejgierd, P.; Patzschke, M.; Pyykkö, P. *J. Chem. Phys.* **2008**, *128*, 224303.
(27) Pyykkö, P.; Zaleski-Ejgierd, P. *J. Chem. Phys.* **2008**, *128*, 124309.
(28) *Handbook of Chemistry and Physics*, 80th ed.; Lide, D. R., Ed.; CRC Press: Boca Raton, 1999.
(29) Pyykkö, P.; Zhao, Y.-F. *J. Phys. Chem.* **1990**, *94*, 7753–7759.
(30) Wannere, C. S.; Corminboeuf, C.; Wang, Z.-X.; Wodrich, M. D.; King, R. B.; Schleyer, P. v. R. *J. Am. Chem. Soc.* **2005**, *127*, 5701–5705.
(31) Pichierri, F. *Mater. Trans.* **2008**, *49*, 2437–2440.
(32) Lin, Y.-C.; Sundholm, D.; Juselius, J.; Cui, L.-F.; Li, X.; Zhai, H.-J.; Wang, L.-S. *J. Phys. Chem. A* **2006**, *110*, 4244–4250.
(33) Furche, F.; Ahlrichs, R.; Weis, P.; Jacob, C.; Gilb, S.; Bierweiler, T.; Kappes, M. M. *J. Chem. Phys.* **2002**, *117*, 6982–6990.
(34) Volkova, L. M.; Magarill, C. A. *Zh. Strukt. Khim.* **1999**, *40*, 314–323.

JP810423J